Periodic boundary layer near an axisymmetric stagnation point on a circular cylinder

Rama Subba Reddy Gorla, Frank Jankowski* and David Textor†
Department of Mechanical Engineering, Cleveland State University,
Cleveland, OH 44115, USA

Received December 1986 and accepted for publication July 1987

An analysis is presented to investigate the time-mean characteristics of the laminar boundary layer near an axisymmetric stagnation point when the velocity of the oncoming flow relative to the body oscillates. Different solutions are obtained for the small and high values of the reduced frequency parameter. The range of Reynolds numbers considered was from 0.01 to 100. Numerical solutions for the velocity functions are presented, and the wall values of the velocity gradients are tabulated.

Keywords: periodic boundary layer, circular cylinder, axisymmetric stagnation point

Introduction

Lighthill[1] studied the effect of fluctuating oncoming stream on the skin friction and heat transfer of a two-dimensional body. He used the results of the velocity field in which the mainstream velocity fluctuates in magnitude but not in direction. Mori and Tokuda[2] investigated the heat transfer from an oscillating cylinder. Gorla[3] examined the unsteady fluid dynamic characteristics of an axisymmetric stagnation point flow on a circular cylinder performing a harmonic motion in its own plane. He presented solutions for small and high values of the reduced frequency of oscillation.

Studies of boundary layer response to an oscillatory flow superimposed on a mean free stream fluid motion are of fundamental importance in many aerodynamic and industrial applications. Typical problems arise in the study of aircraft response to atmospheric gusts, in aerofoil lift hysteresis at the stall, in the prediction of flow over helicopter rotor blades, and through turbomachinery blade cascades.

The present work deals with the time-mean characteristics of the periodic boundary layer near an axisymmetric stagnation point on a circular cylinder. The analysis considers the case when the fluctuations in the external flow are produced by fluctuations of the oncoming stream. Figure 1 shows a cylinder described by $r=a$ in cylindrical polar coordinates. The flow is axisymmetric about the z axis and also symmetric to the $z=0$ plane. The stagnation line is at $z=0$, $r=a$. This flow is useful in certain cooling processes. Gorla[5,6] has recently studied the problem of transient thermal response of a laminar boundary layer in the vicinity of an axisymmetric stagnation flow on an infinite circular cylinder.

Governing equations

Let us consider a laminar, incompressible, unsteady flow at an axisymmetric stagnation point on a circular cylinder. Figure 1 shows the flow model and the coordinate system. The governing equations within boundary layer approximation are as follows:

Mass

$$r\frac{\partial w}{\partial z}+\frac{\partial (ru)}{\partial r}=0 \tag{1}$$

Momentum

$$\frac{\partial u}{\partial t}+u\frac{\partial u}{\partial r}+w\frac{\partial u}{\partial z}=-\frac{1}{\rho}\frac{\partial p}{\partial r}+\nu\left[\frac{\partial^2 u}{\partial r^2}+\frac{1}{r}\frac{\partial u}{\partial r}-\frac{u}{r^2}\right] \tag{2}$$

$$\frac{\partial w}{\partial t}+u\frac{\partial w}{\partial r}+w\frac{\partial w}{\partial z}=-\frac{1}{\rho}\frac{\partial p}{\partial z}+\nu\left[\frac{\partial^2 w}{\partial r^2}+\frac{1}{r}\frac{\partial w}{\partial r}\right] \tag{3}$$

The boundary conditions are given by

$$\begin{aligned} r=a: &\quad u=w=0 \\ r\to\infty: &\quad u=U_e=-A(r-a^2/r)(1+\varepsilon e^{i\Omega t}) \\ &\quad w=W_e=2AZ(1+\varepsilon e^{i\Omega t}) \end{aligned} \tag{4}$$

When ε is small compared with unity, u and w may be expanded as

$$\begin{aligned} u(r,z,t)&=u_0(r,z)+\varepsilon u_1(r,z,t)+\varepsilon^2 u_2(r,z,t)+\cdots \\ w(r,z,t)&=w_0(r,z)+\varepsilon w_1(r,z,t)+\varepsilon^2 w_2(r,z,t)+\cdots \end{aligned} \tag{5}$$

Substituting the expressions in Equation 5 into Equations 1–3 and equating terms of the same order of ε, we obtain sets of

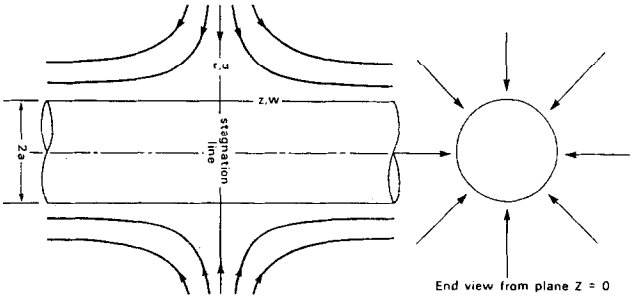

Figure 1 Coordinate system and flow development

*Cleveland Electric Illuminating Company, Cleveland, Ohio
†Diamond Shamrock Corporation, Cleveland, Ohio

differential equations. The zeroth-order equations are

$$r\frac{\partial w_0}{\partial z}+\frac{\partial (ru_0)}{\partial r}=0 \tag{6}$$

$$u_0\frac{\partial u_0}{\partial r}+w_0\frac{\partial u_0}{\partial z}=A^2\left(r-\frac{a^2}{r}\right)\left(1+\frac{a^2}{r^2}\right)+\nu\left[\frac{\partial^2 u_0}{\partial r^2}+\frac{1}{r}\frac{\partial u_0}{\partial r}-\frac{u_0}{r^2}\right] \tag{7}$$

$$u_0\frac{\partial w_0}{\partial r}+w_0\frac{\partial u_0}{\partial z}=4A^2Z+\nu\left[\frac{\partial^2 w_0}{\partial r^2}+\frac{1}{r}\frac{\partial w_0}{\partial r}\right] \tag{8}$$

The boundary conditions for the zeroth-order equations may be written as

$$\begin{aligned} &r=a: && u_0=w_0=0\\ &r\to\infty: && u_0\to -A(r-a^2/r)\\ & && w_0\to 2AZ \end{aligned} \tag{9}$$

The first-order equations are

$$r\frac{\partial w_1}{\partial z}+\frac{\partial}{\partial r}(ru_1)=0 \tag{10}$$

$$\frac{\partial u_1}{\partial t}+u_0\frac{\partial u_1}{\partial r}+u_1\frac{\partial u_0}{\partial r}+w_0\frac{\partial u_1}{\partial z}+w_1\frac{\partial u_0}{\partial z}=-A\left(r-\frac{a^2}{r}\right)i\Omega e^{i\Omega t}+2A^2\left(r-\frac{a^2}{r}\right)\left(1+\frac{a^2}{r^2}\right)e^{i\Omega t}+\nu\left[\frac{\partial^2 u_1}{\partial r^2}+\frac{1}{r}\frac{\partial u_1}{\partial r}-\frac{u_1}{r^2}\right] \tag{11}$$

$$\frac{\partial w_1}{\partial t}+u_0\frac{\partial w_1}{\partial r}+u_1\frac{\partial w_0}{\partial r}+w_0\frac{\partial w_1}{\partial z}+w_1\frac{\partial w_0}{\partial z}=2AZi\Omega e^{i\Omega t}+8A^2Ze^{i\Omega t}+\nu\left[\frac{\partial^2 w_1}{\partial r^2}+\frac{1}{r}\frac{\partial w_1}{\partial r}\right] \tag{12}$$

The boundary conditions for the first-order equations are

$$\begin{aligned} &r=a: && u_1=w_1=0\\ &r\to\infty: && u_1\to -A(r-a^2/r)e^{i\Omega t}\\ & && w_1\to 2AZe^{i\Omega t} \end{aligned} \tag{13}$$

Coordinate transformation and solution

We now define

$$\eta=(r/a)^2$$

$$\begin{aligned} u_0&=-Aa\eta^{-1/2}f(\eta)\\ w_0&=2Af'(\eta)Z\\ u_1&=-Aa\eta^{-1/2}g(\eta)e^{i\Omega t}\\ w_1&=2Ag'(\eta)e^{i\Omega t}\\ \sigma&=\Omega/A\\ \mathrm{Re}&=(Aa^2/2\nu) \end{aligned} \tag{14}$$

Substituting the expressions in Equation 14 into the zeroth-order equations, we have

$$\eta f'''+f''+\mathrm{Re}[1+ff''-(f')^2]=0 \tag{15}$$

The primes designate differentiation with respect to η only. The transformed boundary conditions are

$$f(1)=f'(1)=0 \quad \text{and} \quad f'(\infty)=1 \tag{16}$$

The numerical solution for Equation 15 is well known (see Reference 3), so details are not repeated here.

After substituting Equation 14 into the first-order equations, we have

$$\eta g'''+\tfrac{3}{2}g''+\mathrm{Re}[fg''+gf''-2f'g'+2]+\frac{\mathrm{Re}(1-g')}{2}i\sigma=0 \tag{17}$$

with transformed boundary conditions

$$g(1)=0,\ g'(1)=0, \quad \text{and} \quad g'(\infty)=1 \tag{18}$$

Since Equation 17 contains the frequency parameter α, solutions are presented for small- and large-frequency cases.

Small-frequency case

When $\sigma\ll 1$, we assume that

$$g(\eta)=g_0(\eta)+i\sigma g_1(\eta)+(i\sigma)^2g_2(\eta)+\cdots \tag{19}$$

Substituting Equation 19 into Equation 17 and collecting like powers of $i\sigma$, we have

$$\eta g_0'''+\tfrac{3}{2}g_0''+\mathrm{Re}[fg_0''+g_0f''-2f'g_0'+2]=0 \tag{20}$$

$$\eta g_1'''+\tfrac{3}{2}g_1''+\mathrm{Re}[fg_1''+g_1f''-2f'g_1'+\tfrac{1}{2}(1-g_0')]=0 \tag{21}$$

$$\eta g_2'''+\tfrac{3}{2}g_2''+\mathrm{Re}[fg_2''+g_2f''-2f'g_2'-\tfrac{1}{2}(g_1')]=0 \tag{22}$$

$$\eta g_3'''+\tfrac{3}{2}g_3''+\mathrm{Re}[fg_3''+g_3f''-2f'g_3'-\tfrac{1}{2}(g_2')]=0 \tag{23}$$

$$\eta g_4'''+\tfrac{3}{2}g_4''+\mathrm{Re}[fg_4''+g_4f''-2f'g_4'-\tfrac{1}{2}(g_3')]=0 \tag{24}$$

$$\vdots$$

Equations 20–24 are solved by means of the fourth-order Runge-Kutta numerical procedure on an IBM 370 computer. Re was treated as a prescribable parameter and ranged from

Notation

A	Constant used in Equation 4
a	Radius of cylinder
f, g	Velocity profile functions
p	Pressure
Re	Reynolds number, $Aa^2/2\nu$
r	Coordinate normal to the cylindrical surface
t	Time
u	Velocity component in r direction
w	Velocity component in z direction
z	Coordinate parallel to the wall
η	Dimensionless coordinate
μ	Dynamic viscosity
ν	Kinematic viscosity
ρ	Fluid density
Ω	Frequency of oscillation
σ	Reduced frequency parameter, Ω/A
ε	Amplitude of oscillating velocity

Subscripts

w	Conditions at the wall
∞	Conditions far away from the wall

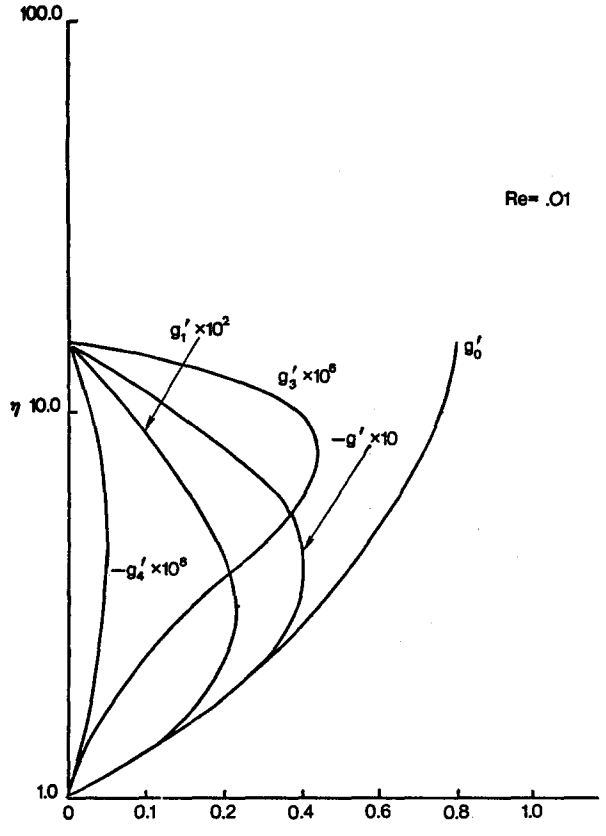

Figure 2 Distribution of g_0', g_1', g_2', g_3' and g_4' for Re = 0.01

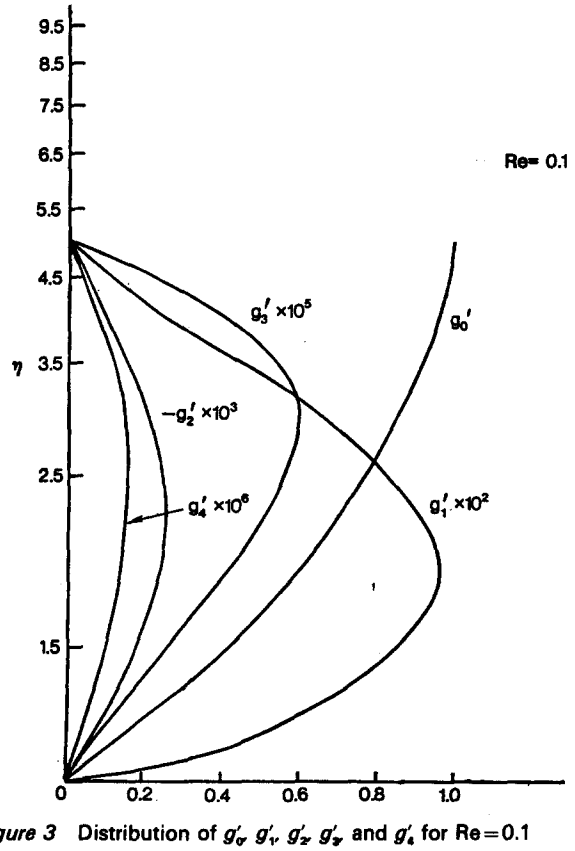

Figure 3 Distribution of g_0', g_1', g_2', g_3' and g_4' for Re = 0.1

0.01 to 100. The numerical results obtained for $g_0'(\eta)$, $g_1'(\eta)$, $g_2'(\eta)$, $g_3'(\eta)$, and $g_4'(\eta)$ are shown in Figures 2–6 for several values of Re. The values of $f''(1)$, $g_0''(1)$, $g_1''(1)$, $g_2''(1)$, $g_3''(1)$, and $g_4''(1)$ for the same range of Reynolds numbers have been tabulated in Table 1. In many practical applications, a knowledge of the wall shear stress is of importance and may be calculated by using the information in Table 1. The local wall shear stress may be written as

$$\tau_w = \mu\left(\frac{\partial w}{\partial r}\right)_{r=a}$$

$$= \mu\frac{4AZ}{a}[f''(1)+\varepsilon e^{i\Omega t}g''(1)+\cdots] \tag{25}$$

Defining

$$\tau_{wo} = \mu\left.\frac{\partial \omega_0}{\partial r}\right|_{r=a}$$

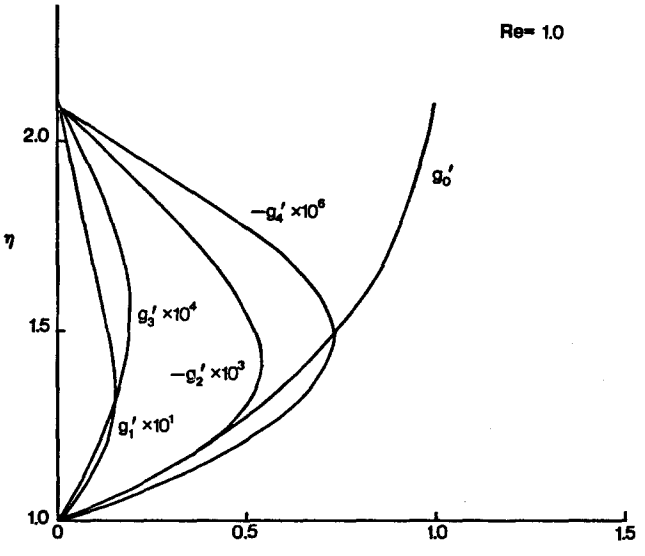

Figure 4 Distribution of g_0', g_1', g_2', g_3' and g_4' for Re = 1.0

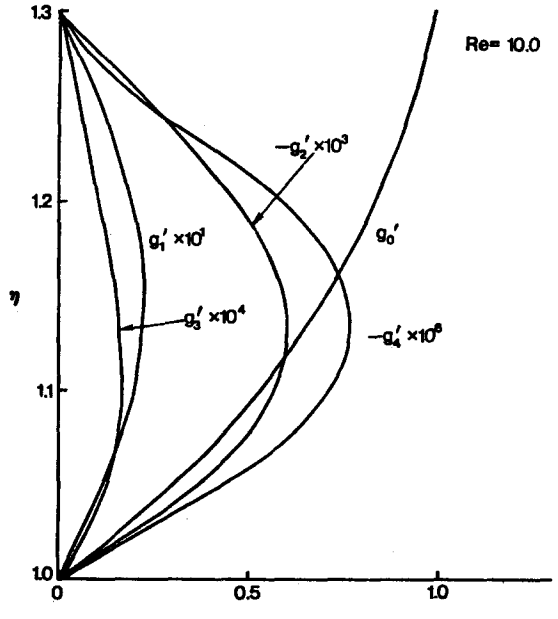

Figure 5 Distribution of g_0', g_1', g_2', g_3' and g_4' for Re = 10.0

and

$$\tau_{wt}=\mu\left.\frac{\partial w_1}{\partial r}\right|_{r=a}$$

we may write

$$\frac{\tau_{wt}}{\tau_{wo}}=\frac{1}{f''(1)}[g_0''(1)+(i\sigma)g_1''(1)+(i\sigma)^2g_2''(1)+(i\sigma)^3g_3''(1)+(i\sigma)^4g_4''(1)+\cdots] \tag{26}$$

High-frequency case

For this case we assume that

$$g=P(\eta,\sigma)+Q(\sigma)e^{R(\eta,\sigma)} \tag{27}$$

where

$$P=P_0(\eta)+\frac{P_1(\eta)}{\sqrt{\sigma}}+\frac{P_2(\eta)}{\sigma}+\frac{P_3(\eta)}{\sigma^{3/2}}+\cdots$$

$$Q=Q_0+\frac{Q_1}{\sqrt{\sigma}}+\frac{Q_2}{\sigma}+\frac{Q_3}{\sigma^{3/2}}+\cdots$$

$$R=\sqrt{\sigma}\left[R_0(\eta)+\frac{R_1(\eta)}{\sqrt{\sigma}}+\frac{R_2(\eta)}{\sigma}+\cdots\right] \tag{28}$$

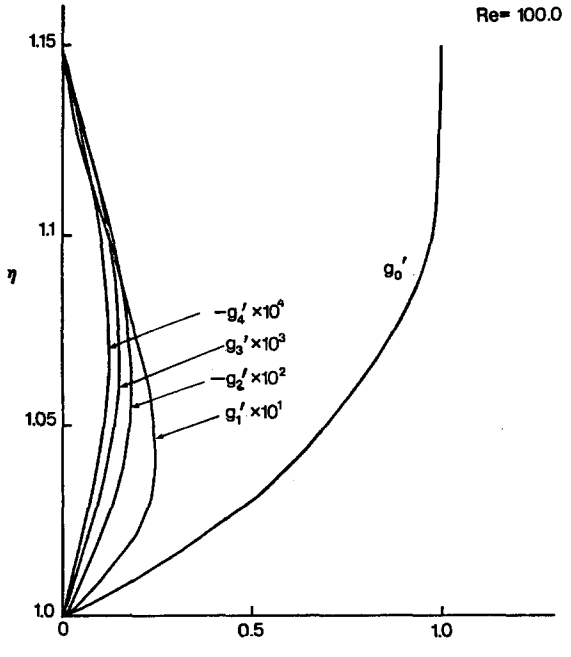

Figure 6 Distribution of g_0', g_1', g_2', g_3' and g_4' for Re = 100.0

Substituting Equations 27 and 28 into Equation 17, we obtain

$$P_0'-1=0$$

$$P_1'=0$$

$$iP_0''=\frac{2}{\mathrm{Re}}\{\eta P_0'''+(\tfrac{3}{2}+\mathrm{Re}\,f)P_0''+\mathrm{Re}\,f''P_0-2\,\mathrm{Re}\,f'P_0+2\,\mathrm{Re}\}$$

$$iR_0'-\frac{2}{\mathrm{Re}}\eta(R_0')^3=0$$

$$iR_1'=\frac{6}{\mathrm{Re}}\eta(R_0')^2R_1'\times\frac{6}{\mathrm{Re}}R_0'R_0''+\frac{2}{\mathrm{Re}}(\tfrac{3}{2}+\mathrm{Re}\,f)(R_0')^2$$

$$\vdots \tag{29}$$

The boundary conditions are

$$P_0(1)=0$$

$$P_1(1)+Q_0=0$$

$$P_0'(1)+R_0'(1)(Q_0)=0$$

$$P_1'(1)+Q_0R_1'(1)Q_1=0$$

$$\vdots \tag{30}$$

It may be finally shown that

$$g(\eta)=\left[(\eta-1)-\left(\frac{2}{\mathrm{Re}}\right)^{1/2}\frac{1}{\sqrt{i\sigma}}+\cdots\right]+\left[\left(\frac{2}{\mathrm{Re}}\right)^{1/2}\frac{1}{\sqrt{i\sigma}}+\cdots\right]\exp(R) \tag{31}$$

where

$$R=-\sqrt{2\,\mathrm{Re}}\sqrt{i\sigma}\,(\eta^{1/2}-1)-\left[\frac{3}{4}\left(\frac{1}{\eta}-1\right)+\frac{3}{4}\ln\eta+\frac{\mathrm{Re}}{2}\int_1^\eta\frac{f}{\eta}\,d\eta\right]$$

Using Equations 30 and 25, we may write

$$\frac{\tau_{wt}}{\tau_{wo}}=\frac{1}{f''(1)}\left[\frac{1}{2}+\sqrt{\frac{\mathrm{Re}}{2}}\sqrt{i\sigma}-\frac{3}{4}\sqrt{\frac{2}{\mathrm{Re}}}\frac{1}{\sqrt{i\sigma}}+\cdots\right] \tag{32}$$

The amplitude C and phase angle ϕ of the fluctuating skin friction of order ε have been illustrated in Figures 7–9 for selective values of the Reynolds number.

Discussion

The magnitude of the shear stress may be calculated from Equation 32 as follows:

$$|\tau_w|=[(\tau_w)_R^2+(\tau_w)_I^2]^{1/2} \tag{33}$$

The phase angle for the shear stress is

$$\phi_M=\tan^{-1}[(\tau_w)_I/(\tau_w)_R] \tag{34}$$

In the above equations, the subscripts I and R denote imaginary and real parts, respectively.

Table 1 Values of $\mathrm{Re}^{-1/2}f''(1)$ and $\mathrm{Re}^{-1/2}g_n(1)$ for various values of Re

Re	$\mathrm{Re}^{-1/2}f''(1)$	$\mathrm{Re}^{-1/2}g_0''(1)$	$\mathrm{Re}^{-1/2}g_1''(1)$	$\mathrm{Re}^{-1/2}g_2''(1)$	$\mathrm{Re}^{-1/2}g_3''(1)$	$\mathrm{Re}^{-1/2}g_4''(1)$
0.01	3.155182	7.559609	0.082588	−0.000810	1.0412×10^{-6}	-1.1×10^{-7}
0.10	1.946369	3.726076	0.105598	−0.001803	1.2645×10^{-6}	-9.648×10^{-7}
1.00	1.484185	2.475295	0.118451	−0.002611	5.3851×10^{-5}	-2.9741×10^{-6}
10.10	1.316427	2.095865	0.119579	−0.002629	2.4222×10^{-4}	-3.0157×10^{-6}
100.00	1.259642	1.911631	0.140150	−0.005480	3.61606×10^{-4}	-3.07083×10^{-5}

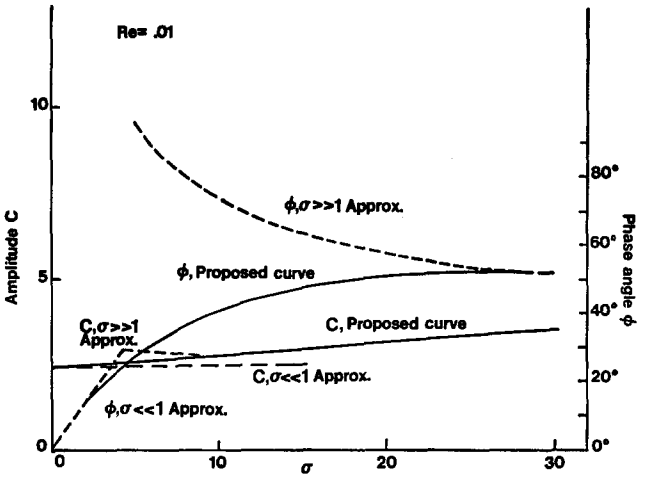

Figure 7 Amplitude C and phase angle ϕ of the fluctuating component of skin friction for Re = 0.01

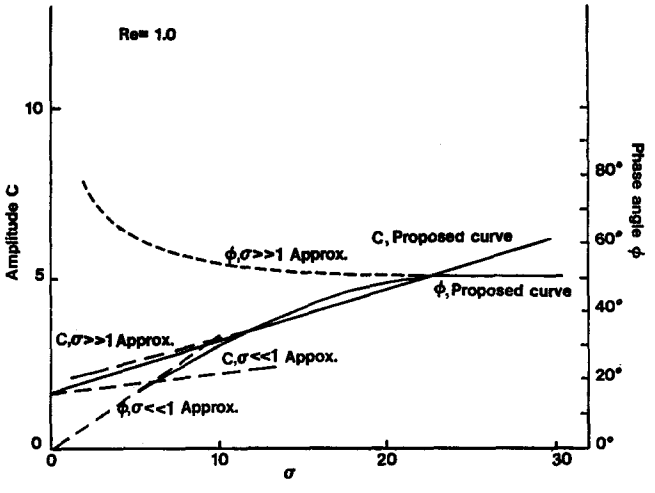

Figure 8 Amplitude C and phase angle ϕ of the fluctuating component of skin friction for Re = 1.0

Figures 2–6 show the numerical results for the first-order unsteady equations for Re ranging from 0.01 to 100.

Figures 7–9 display the results for the amplitude and phase angle of the wall skin friction fluctuations. In these figures, the low-frequency solution and the high-frequency solution are shown by dotted lines, and the solid curves represent the matching of these asymptotic solutions. The amplitude of the skin friction fluctuation increases monotonically with the dimensionless frequency parameter σ.

The phase angle is in advance of the free stream fluctuation and an asymptotic phase advace of 50° is attained for the range of Reynolds numbers investigated. For $\mathrm{Re}\to\infty$, it was noticed that this phase advance approaches 45° at very large frequency. The low-frequency solution does not always agree with the high-frequency solution near the region where the frequency parameter is unity, but the solution truncated at the fifth power for low frequency agrees well with the one truncated at the third power for high frequency in that region.

We expect that the results for large values of Re would correspond to the two-dimensional stagnation flow on a flat plate. Using the transformation

$$f(\eta)=\mathrm{Re}^{-1/2}\phi(\xi), \qquad \xi=\mathrm{Re}^{1/2}(\eta-1) \tag{35}$$

we can see that Equation 15 reduces to the Hiemenz problem

$$\phi'''+\phi\phi''-(\phi')^2+1=0 \tag{36}$$

with boundary conditions

$$\phi(0)=\phi'(0)=0, \qquad \phi'(\infty)=1 \tag{37}$$

Similarly by defining

$$g(\eta)=\mathrm{Re}^{-1/2}h(\eta) \tag{38}$$

we find that Equation 17 reduces to

$$h''+\phi h'-h\phi'-i\sigma h=0 \tag{39}$$

with boundary conditions

$$h(0)=0, \qquad h(\infty)=1 \tag{40}$$

For $\sigma=0$, Equation 37 yields

$$h=\phi''(\eta)/\phi''(0)=0.811\phi''(\eta) \tag{41}$$

Concluding remarks

The velocity distribution in an oscillating laminar boundary layer in the vicinity of an axisymmetric stagnation point has been analyzed by means of a boundary layer approximation. The amplitude and the phase angle of the wall skin friction fluctuation are calculated for small and large values of the reduced frequency of oscillation.

The results indicate that the amplitude and phase advance of skin friction fluctuation increase with frequency of oscillation of the mainstream, and an asymptotic phase advance of 50° is attained at very large frequency for Reynolds numbers ranging from 0.01 to 10. For $\mathrm{Re}\to\infty$, this phase advance was observed to reach 45°.

The flow configuration described in this paper finds its applications in certain cooling processes as well as quenching. The analysis presented in the paper should help in the understanding of the flow mechanism and in an estimate of friction loss.

Acknowledgments

This work has been supported through the cooperative agreement No. NCC3-3 by NASA Lewis Research Center. R. S. R. Gorla is grateful to Dr. Robert J. Simoneau and Dr. Robert W.

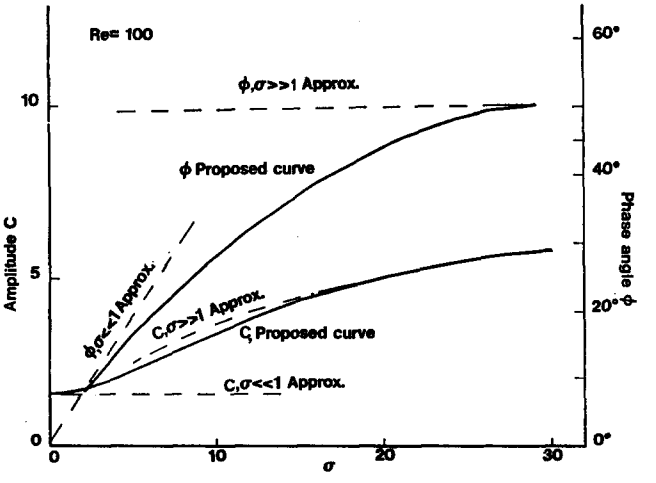

Figure 9 Amplitude C and phase angle ϕ of the fluctuating component of skin friction for Re = 100.0

Graham of the NASA Lewis Research Center for their interest and encouragement.

References

1 Lighthill, M. J. The response of laminar skin friction and heat transfer to fluctuations in the stream velocity. *Proc. Roy. Soc.*, 1954, **224**(A), 1–23

2 Mori, Y. and Tokuda, S. The effect of oscillation in instantaneous local heat transfer in forced convection from a cylinder. Proc. Third Int. Heat Transfer Conference, Vol. 3, 1966, 46–56

3 Gorla, R. S. R. Unsteady viscous flow in the vicinity of an axisymmetric stagnation point on a circular cylinder. *Int. J. Engng. Sci.*, 1979, **10**, 87–93

4 Gorla, R. S. R. The final approach to steady state in a non-steady axisymmetric stagnation point heat transfer. *J. Warme- und Stoffubertragung*, 1987, 21

5 Gorla, R. S. R. Transient response behavior of an axisymmetric stagnation flow on a circular cylinder due to the time dependent free stream velocity. *Int. J. Engng. Sci.*, 1978, **16**, 493–502

6 Gorla, R. S. R. Nonsimilar axisymmetric stagnation flow on a moving cylinder. *Int. J. Engng. Sci.*, 1978, **16**, 397–400